

# MOTION DETECTION MECHANISMS

Bart Krekelberg

## Full Address

**Bart Krekelberg**  
Center for Molecular and Behavioral Neuroscience  
Rutgers University  
197 University Avenue  
Newark, NJ 07102  
T: +1 973 353 1080 X3231  
F: +1 973 353 1272  
E: bart@rutgers.edu

## Address For Publication.:

Center for Molecular and Behavioral Neuroscience  
Rutgers University  
197 University Avenue  
Newark, NJ 07102  
E: bart@rutgers.edu

## Keywords

Motion, Perception, Reichardt Detector, Motion Energy Model, Gradient Model, Visual Cortex, Insect Vision, Cat, Monkey, Computational Neuroscience

## Synopsis

This review discusses theoretical, behavioral, and physiological studies of motion mechanisms. The three main schemes for motion detection (space-time correlation, orientation, and gradients) are contrasted using experimental data from insects, rabbits, cats, monkeys, and humans. These schemes provide a basic understanding of the organization of many neural motion detection systems. However, few neural systems are pure implementations of any of these three detection schemes. It is suggested that using a mixture of motion detection mechanisms may be advantageous to a neural system faced with the difficult, but important task of detecting motion under widely varying conditions.

*Like beauty and color, motion is in the eye of the beholder.*

## **1 INTRODUCTION**

The physical phenomenon ‘motion’ can easily be defined as an object’s change in position over time. An animal that can detect moving predators, prey, and mates, has a clear survival advantage and this evolutionary pressure has presumably led to the development of neural mechanisms sensitive to motion. However, the combined effect of evolutionary circumstance, conflicting demands on the perceptual apparatus, and limitations of biological hardware, have led to motion detection mechanisms that are far from perfect. A neural motion detection mechanism may not respond appropriately to all kinds of changes in position, and it may respond to some inputs that are not changes in position at all. It is in this sense that I subscribe to the quote from Watson and Ahumada (1985) at the start of this chapter; (the percept of) motion is constructed by the beholder’s imperfect mechanisms for the detection of (physical) motion. The goal of this chapter is first to elucidate the principles that the brain relies on to detect motion. But second, to point out that strict adherence to those principles is quite rare, and that imperfect implementations are the rule, rather than the exception.

Research into motion detection mechanisms is strongly model-driven. Many studies are guided by particular views of the computations that are needed to detect motion; they aim to uncover the algorithms used by the brain, and describe the details of the neural implementations (Marr, 1982). Before delving into the details of motion detection mechanisms, I will give a brief bird’s eye view of motion detection along these lines.

**Computations.** Three views of the computations required for motion detection have emerged (Figure 2). The first states that to detect motion one needs to compute whether the presence of light at one position is later followed by light at another position. To detect motion, light has to be detected at both positions and times, and then compared. In the second view of motion, it is a continuous process of change. This view states that a moving object traces out an oriented light distribution in space-time (see Figure 1). To detect motion, one needs to measure this orientation. The third view starts from the observation that motion can only be observed when there is both a temporal and a spatial change in light intensity. To detect motion, both need to be measured and compared. Each of these views suggests a different emphasis on algorithms that are relevant to compute motion.

**Figure 1** Motion as space-time orientation. A) When a bar moves smoothly rightward over time, it traces out an oriented trapezoid in a space-time plot. B) When that same bar jumps from one place to the next (apparent motion), the space-time orientation is still clearly visible.

**Algorithms.** The computations required by the first view can be performed by detecting light in the first position, delaying the signal, and multiplying it with the signal arising from the (undelayed) signal arising from the detector in the second position. This algorithm essentially performs a space-time auto-correlation. The computations of the second view require an estimate of space-time slant. This can be done by convolving the image with filters that are oriented in space-time. The computations of the third view require the estimation of both the spatial and temporal gradients in light intensity of an image. In abstract terms, such gradients can be determined by convolving the image with

appropriate (differentiating) filters. The motion signal is then given by the ratio of the temporal and spatial gradients. Each of these algorithms requires different neural hardware for its implementation.

**Figure 2 Three views of motion detection.** A) The Reichardt detector makes use of sensors that are displaced in space and time with respect to each other. By multiplying their outputs (indicated by the arrows), one can create a rightward (R) or leftward (L) selective detector. B) The motion energy detector uses overlapping sensors that are sensitive to rightward (R) or leftward (L) space-time slant. C) The gradient detector uses overlapping detectors, sensitive to either spatial (S) or temporal (T) change. Adapted from (Johnston and Clifford, 1995b).

**Implementations.** In the space-time correlation view, temporal delays and multiplication are the essential ingredients to detect motion. While temporal delays are part and parcel of neural responses, multiplication of two signals is not as straightforward. Much of the research at the implementation level is therefore devoted to understanding if and how neurons can perform a multiplication. In the space-time orientation view, neurons space time response maps must be slanted. Research in this tradition therefore concentrates on measuring detailed properties of space time response maps. In the space-time gradient view, neuron's space time response maps should match those of differentiating filters. Research in this tradition looks for such properties in visual neurons.

I will use these three views of motion detection (Correlation, Orientation, and Gradients) as the skeleton to organize this chapter. It should be noted, however, that they are not mutually exclusive or even entirely independent. In fact, under some assumptions about the visual input, the detectors based on the three views become formally identical at their

output levels (van Santen and Sperling, 1985, Adelson and Bergen, 1985, Bruce et al., 2003). On the other hand, these formal proofs should not be misconstrued to imply that the three computations, algorithms and implementations are “all the same”. Behavioral methods may be hard-pushed to distinguish among some of the models because they only have access to the output of the motion detection mechanisms. But, as we will see, neurophysiological methods can gain access to intermediate steps in the computations which are distinct.

My goal is to present some of the salient evidence in favor of the Correlation, Orientation, or Gradient models. At the same time, however, I believe it is important to realize that the brain may not perform any of these computations perfectly. Such imperfections may have arisen from competing constraints in the evolution of the visual system, or the limitations of biological hardware. As such, imperfections may be a nuisance in a model of motion detection, but in fact, they can be instructive in the larger view of the organization of the brain.

Sections 3, 4, and 5 review the literature on correlation, orientation, and gradient models respectively. Before delving into the literature, however, I first discuss some of the methods and terminology that have proven useful in the study of motion detection.

## **2 RESEARCH IN MOTION**

Motion mechanisms can be studied by comparing the (behavioral or neural) response to a stimulus moving in one direction with that same stimulus moving in another direction. For direction selective neurons, this is often reduced to responses to a stimulus moving in the preferred and the opposite, anti-preferred direction. Many studies use sinusoidal

gratings as the stimulus. The reason for using gratings is that, as long as a neuron (or mechanism) is well described as a linear system, the response to sinusoidal gratings can be used to predict the response to an arbitrary stimulus (Movshon et al., 1978b, Movshon et al., 1978a). This Fourier analysis is only truly applicable to linear systems, which neurons in general and direction selective neurons in particular are not. Nevertheless, the Fourier method has proven to be useful and much of the terminology in the field is derived from it.

To study the internal mechanisms of a motion detector, a sinusoidal grating, may not always be the best choice. Although somewhat counterintuitive at first, even moving stimuli may not be the optimal stimuli to study motion mechanisms. The reason for this is that any motion mechanism worth considering would predict that motion in the preferred direction evokes a larger response than motion in the anti-preferred direction. Hence, finding such responses does not tell us much about the internal mechanisms of the detector.

Many studies use flashed stimuli to characterize the response of motion detection mechanisms. A single flash by definition does not contain a motion signal, but nevertheless, it often activates motion detectors (and therefore may even appear to move). The minimal true motion signal is generated by two successive flashes. Thus, by comparing the response of a motion detector to two successive flashes with the response evoked by those same flashes presented in isolation, one can extract motion-specific response properties.

A further elaboration of this technique leads to the white noise analysis of nonlinear systems identification (Marmarelis and Marmarelis, 1978). In this approach, the stimulus is a noisy pattern whose intensity varies rapidly and randomly. One can view this as a stimulus with multiple flashes occurring at the same time. Given enough time, all possible patterns will be presented to the detector, the responses to all possible patterns will be recorded, and the complete input-output relationship can be determined. In the finite time available for an experiment one can of course only approximate this situation. Typically these approximations take into account the first order response (response to a flash at a particular position) and the second order response (interaction between two flashes separated in space and time).

With these methods it is possible to measure the properties that have proven to be useful to describe motion detection mechanism and that will recur throughout this chapter:

- Direction Selectivity: a comparison between the responses to two stimuli moving in opposite directions.
- Space-time response map (RF): the response to a flash at some position in the cells receptive field, presented at time zero, measured at time  $t$ . Because I will only consider one-dimensional motion, the space-time response map is two-dimensional.
- Space-time interaction map: the response enhancement observed for a stimulus presented at  $(t_1, x_1)$ , when another stimulus has already been presented at  $(t_2, x_2)$ . This is a four dimensional map. Often, however, the relative, not the absolute time and position of the flashes matter. In such cases, the interaction map becomes two

dimensional and represents the enhancement in the response to a flash due to the presentation of another flash  $dt$  earlier and at a distance of  $dx$ .

In the sections that follow, these measures of the internal properties of a motion detector will be used extensively to characterize experimental data, and to distinguish between models.

### 3 SPACE-TIME CORRELATION

The study of the neural mechanisms of motion detection started in earnest with work on insects by Hassenstein, Reichardt and Varju, in the early 1950's. Considering the faceted eyes of insects, it is natural to view motion as the detection of successive activation of neighboring ommatidia.

#### 3.1 THE REICHARDT DETECTOR

Hassenstein and Reichardt (1956) proposed the first formal model of motion detection on the basis of careful observations of the behavior of the beetle (*Chlorophanus Viridis*). When placed in a moving environment, this beetle has the instinctive reaction to turn with the motion of the environment. Presumably it does this to keep moving in a direction that is constant with respect to the environment. Later studies have made use of similar optomotor responses in houseflies, blow flies, and locusts to gain access to their percept of motion.

**Figure 3 A beetle on a *Spangenglobus*. The beetle is glued to the black pole which holds it stationary in space. When it is lowered onto the y-maze globe, it instinctively grabs it and starts “walking” along the ridges. When it comes to a y-junction, it must make a decision to go right or left. This decision can be influenced by presenting motion in the environment. (© Freiburger Universitaetsblaetter).**



By putting the beetle on a Y-globe (or '*Spangenglobus*', in German), and surrounding it by a cylinder marked with vertical patterns, Hassenstein and Reichardt were able to quantify the beetle's motion percept (Figure 3). For instance, when they first presented a bright (+1) bar such that its light hit a specific ommatidium and then another bright bar to stimulate the nearest ommatidium to the left, the beetle turned towards the left. When a dark (-1) bar was followed by a dark bar on the left, the beetle also turned to the left. But, when a bright (+1) bar followed a dark (-1) bar on the left, the beetle turned to the right. From these key observations, they concluded that a simple algebraic multiplication of the contrasts of the visual patterns could underlie the motion response. Additionally, they found that, for any given two-bar sequence, the optomotor response was strongest when there was about 250 ms between the two stimuli. A simple model that captures both these properties is shown in Figure 4 .

**Figure 4 The (Hassenstein-) Reichardt detector. The light sensors represent the beetle's ommatidia. Signals from two neighboring ommatidia (I) are multiplied at stage III. One of the two input signals, however, is first delayed (II). The output of the multiplication stage in black is selective for rightward motion. This selectivity is enhanced in the last stage (IV) by subtracting the output of a leftward selective subunit (in gray) from that of the rightward selective subunit.**

The first stage represents the input from two neighboring ommatidia. At the second stage, the input from one location is delayed. The third stage implements the multiplication that Hassenstein and Reichardt observed to underlie the beetle's behavior. This is an essential nonlinear operation, without which no direction selectivity could be generated in the

time-averaged signal (Poggio and Reichardt, 1973, Poggio and Reichardt, 1981). To create a signal whose average value indicates the direction of motion, his stage can also average the signal over time. Finally, the output of a leftward selective motion detector is subtracted from that of a rightward detector in the fourth stage. This subtraction greatly improves the selectivity of the detector (Borst and Egelhaaf, 1990). The result is a single valued output that is positive for rightward motion and negative for leftward motion. One could imagine such a number being fed straight into a motor control system to generate the beetle's following response. Formally, one can show that the output of this stage is the autocorrelation of the input signal (Reichardt, 1961). In other words, the detector determines how much a signal in one location is like the signal at a later time at a position to the right. If this autocorrelation is positive, motion is to the right; if it is negative motion is to the left.

## 3.2 *BEHAVIORAL EVIDENCE*

The Reichardt detector makes some very specific and sometimes counterintuitive predictions about motion perception that have been tested in detail. I will highlight a few of these here.

### 3.2.1 *Facilitation*

When a stimulus jumps from one position to the next and increases its contrast at the same time, the Reichardt model predicts that the motion signal is proportional to the product of the pre-jump and post-jump contrast. As long as stimulus contrast is small enough, this is indeed the case in many insects (Reichardt, 1961, McCann and MacGinitie, 1965, Buchner, 1984). For higher contrasts, however, further increases in

contrast no longer strengthen the motion signal. Hence, a complete model should incorporate some kind of saturation or normalization of the response for high contrast.

Van Santen and Sperling (1984) investigated this issue in humans and showed that, at least at low contrast, the motion signal indeed increased as the product of pre- and post-jump contrasts. This clearly argues in favor of facilitation and even suggests that this facilitation takes the form of a multiplication. More recent experiments, however, show that perception is affected differently depending on whether the pre-jump or post-jump stimulus contrast is increased (Morgan and Chubb, 1999). Neither of these effects would be expected in a pure Reichardt detector, but may be explained by adding noise sources and contrast normalization mechanisms to the motion detector (Solomon et al., 2005).

### 3.2.2 *Reverse-phi*

The multiplication in the Reichardt model ensures that motion detection does not depend on the polarity of the contrast of a moving object (dark objects lead to the same motion signals as bright objects). At the same time, however, the multiplication causes a reversal of motion direction for stimuli whose contrast *changes* polarity. This inversion of motion direction with an inversion of contrast polarity during a motion step is called reverse-phi and has been observed behaviorally in insects (Buchner, 1984, Reichardt, 1961), non-human primates (Krekelberg and Albright, 2005), as well as humans (Anstis, 1970, Anstis and Rogers, 1975). This behavioral evidence suggests that the pathways detecting bright (ON) and dark (OFF) onsets interact within the motion system and that this interaction has the signature of a multiplication.

Behavioral evidence in humans, however, suggests that the ON and OFF systems are not treated as symmetrically as envisaged in the Reichardt model. For instance, the direction of motion in a sequence of dark and bright flashes requires a much longer delay to be detectable than a sequence of flashes of the same polarity (Wehrhahn and Rapf, 1992). Moreover, the reverse-phi phenomenon is found for eccentric presentations, but is much reduced near the fovea or when the distance between the observer and the stimulus is increased (Lu and Sperling, 1999).

### *3.2.3 Phase invariance*

The Reichardt detector determines the autocorrelation of an input signal. Because the autocorrelation does not depend on the starting phase of the signal, this implies that for any arbitrary pattern (that can be described as the sum of sinusoidal gratings), replacing one of the component gratings by a phase-shifted grating does not change the output of the detector. This prediction has been confirmed at the behavioral level in the beetle. Reichardt took two (essentially arbitrary) spatial patterns and constructed a first visual stimulus by simple addition of the patterns, and a second visual stimulus by adding the patterns with a spatial phase shift. When a beetle was confronted with these two visual stimuli, its walking behavior on the Spangenglobus was identical. (Reichardt, 1961).

### *3.2.4 Pattern dependence*

While the phase of gratings does not affect the output of the detector, other properties, such as the spatial frequency, do. This shows that the Reichardt detector is not ideal; its output is not the same for every visual stimulus with the same velocity. While suboptimal from the viewpoint of an ideal motion detector, this does provide another counterintuitive

prediction of the Reichardt model. To be precise, the model predicts that for every speed the detector responds only weakly to the lowest spatial frequencies, climbs to a maximum and then declines for higher spatial frequencies. Optomotor responses in many insects are consistent with this prediction (Buchner, 1984).

A more extreme case of mistaken velocity arises from spatial aliasing for high spatial frequencies. When a rightward Reichardt detector is stimulated with a rightward moving grating whose spatial period is smaller than twice the distance between the input channels it will evoke a negative (i.e. leftward) response. While this is clearly an undesirable property for a motion detector, the behavior of the blowfly actually matches this (Zaagman et al., 1976). In other insects, the relationship between the behavioral inversion and receptor spacing is not as clean, although this may be understood by assuming that the detector receives input from more than one neighboring ommatidium (Thorson, 1966b, McCann and MacGinitie, 1965).

Human visual motion perception is also spatial frequency dependent in a manner that is consistent with the Reichardt model (Burr and Ross, 1982, Smith and Edgar, 1990). The inversion of the perceived direction of motion that is observed at high spatial frequencies in insects, however, is not observed in human behavior (van Santen and Sperling, 1984). The simplest way to modify the Reichardt model such that the spatial aliasing no longer occurs, is to remove the affected high spatial frequencies from the input at an early stage. Van Santen and Sperling (1984) proposed the Extended Reichardt model, which has such pre-filters and removes the spatial aliasing behavior. Its flow-chart is shown in Figure 5.

The pre-filters essentially state that the elementary light sensors that provide input to the motion detectors, are not point sensors, but have an (overlapping) spatial extent.

**Figure 5 The extended Reichardt model. Light falling on the retina is spatially (II) and temporally filtered (III). The outputs of the four filters are then pairwise multiplied (Stage IV). As in the standard Reichardt detector, the rightward selective subunit (black) is combined with a mirror symmetric leftward selective subunit (gray), at stage V.**

Interestingly, the pattern dependence in the Reichardt detector arises only at the last subtraction stage. The so-called half-detectors respond to a moving pattern regardless of its spatial frequency. In other words, they are velocity tuned and not spatio-temporal frequency tuned (Zanker et al., 1999). But, as pointed out above, the motion selectivity of such half-detectors is weak (Borst and Egelhaaf, 1990). In a biological system, it seems likely that the subtraction of a leftward and rightward half-detector may not be perfect. This would have the effect of creating detectors that trade-off motion selectivity (fully symmetric subtraction at stage IV) against pattern invariance (No subtraction of opposite motion detectors).

### 3.3 *PHYSIOLOGICAL EVIDENCE*

Many physiological studies have looked for and found neural response properties consistent with the Reichardt detector. Figure 6 shows what the model predicts for experiments that measure the space time response map by presenting single flashes at various positions in a neuron's receptive field. The first four space time response maps represent recordings from neurons at stage III of the extended Reichardt model (Indicated

by A,B,A', and B' in Figure 5 and Figure 6). The defining property of these space-time RFs is that they are not oriented in space time; they are well-described as the product of a spatial and a temporal profile. This separability is also observed at stage IV; here both the left and the rightward subunit are predicted to have the same response to flashed stimuli. As a result, the complete detector, which subtracts the outputs of Left and Right detectors, gives no response at all to single flashes.

**Figure 6 One flash space-time response maps of the Reichardt model.** Each of these plots shows the response of a stage in the extended Reichardt model to the presentation of a single bright flashed stimulus. Time after the stimulus runs down the vertical axis, the position of the stimulus relative to the receptive field center, is on the horizontal axis. Pixels brighter than the gray zero level (see colorbar on the right), represent an increase in the activity, dark pixels represent a decrease in activity. Within the linear model, such a decrease in firing after the presentation of a bright bar is equivalent to an increase in firing after the presentation of a dark bar. The labels in the lower left corner of each space-time response map refer to the labels in Figure 5.

### *3.3.1 Facilitation and suppression*

As can be seen from Figure 6, an ideal Reichardt detector should not respond at all to a single flashed bar. With an ingenious device that allowed them to flash a light on individual photoreceptors of the fly's eye while recording extracellularly from the H1 neuron, Franceschini et al. (1989) provided evidence for this property. Single flashes, whether dark or bright, did not evoke a response in the H1 neuron. Such clean Reichardt behavior is rare; typically, motion detectors will respond vigorously to a single flash (Borst and Egelhaaf, 1990). No major modification of the model is required to explain this. For instance, some level of spontaneous activity in the multiplication stage would suffice to allow a strong input to always evoke a significant response. Alternatively, the

subtraction of the left and right subunit outputs may not be perfect. For instance, instead of calculating  $R-L$ , the detector may calculate  $R-\beta L$ , where  $0 < \beta < 1$  (Borst and Egelhaaf, 1990).

The essential prediction of the Reichardt is that the response to two successive flashes – displaced in the preferred direction – is larger than that to two successive flashes displaced in the anti-preferred direction. In other words, by comparing two-flash apparent motion in the preferred and anti-preferred direction, one should observe facilitation and suppression of the neural response, respectively. Model calculations for this facilitation (bright) and suppression (dark) are shown for a rightward Reichardt motion detector in Figure 7.

Franceschini et al. tested this in the H1 neuron of the fly. When two successive flashes to separate photoreceptors simulated forward motion, the second flash evoked a strong response (Franceschini et al., 1989). Presenting these flashes in the opposite order, simulating anti-preferred motion, however, evoked no response or, in a cell with a large spontaneous firing rate, a suppression of the firing rate. This is consistent with the presence of the white (facilitation) and black (suppression) patches around the origin of the interaction map in Figure 7. This was confirmed by Borst and Egelhaaf (1990) who recorded interaction maps for the fly H1 neuron. At low contrast, the preferred direction flashes showed clear facilitation, while the anti-preferred direction flashes showed suppression. The suppression was evident also at high contrast, but the facilitation disappeared. The latter may be explained by a saturation process: if the individual flashes evoke a strong response, their combination in the preferred direction may not lead to any



further enhancements because the response is already near the maximum and saturates. This, again, shows an imperfection in the neural motion detector. While the Reichardt detector predicts a quadratic increase of the response with contrast, real neurons do not have an infinite range and will saturate at some contrast level. This is not a difficult property to incorporate into the model, but uncertainty about the shape of the contrast response function provides additional obstacles to the creation of a quantitative model.

**Figure 7 Two-flash space-time interaction maps of the extended Reichardt model. These interaction maps show which part of the response to two successive flashes is not expected based on the linear summation of the response to the two flashes presented in isolation. The time between the two flashes is on the vertical axis, the distance between the flashes on the horizontal axis. Bright pixels show a facilitating interaction, dark pixels a suppressive interaction.**

In the rabbit retina, the main effect underlying direction selectivity appears to be a suppression for the anti-preferred direction (Barlow and Hill, 1963, Barlow et al., 1964, Amthor and Grzywacz, 1993, Fried et al., 2002), with a smaller contribution from facilitation for two flashes presented in the preferred direction (Grzywacz and Amthor, 1993, Taylor and Vaney, 2002, Fried et al., 2005). This has led to the so-called *veto* model. In this model, the activity of a second flash, presented in the anti-preferred direction, is inhibited ('vetoed') by the presentation of the first flash. The requirements for this model are very similar to those of the Reichardt model. Notably, the first flash must be able to evoke suppression at a later time (i.e. a delay is needed). Later work has shown that a multiplicative nonlinearity may implement this veto mechanism (Torre and Poggio, 1978), see Section 3.3.3.

### 3.3.2 *Reverse-phi*

The Reichardt model predicts that an inversion of the contrast of a two-flash stimulus leads to an inversion of directional preference.

Franceschini et al. (1989) investigated this by stimulating individual photoreceptors and found that there is more facilitation between flashes of the same contrast polarity than between flashes of opposite polarity. Thus they argue for some level of separation between the ON and OFF pathways. A later study, however, showed clear evidence of reverse-phi in the fly H1 cell: suppression is observed when a bright-dark two-flash stimulus is presented in the preferred direction, and facilitation is seen for a bright-dark two-flash stimulus presented in the anti-preferred direction (Egelhaaf and Borst, 1992). While not entirely resolved, this discrepancy may have been due to response saturation at the high contrasts used in the earlier studies. Alternatively, this could be a reflection of the small sample size of the earlier studies (Franceschini et al., 1989, Horridge and Marcelja, 1991) and the fact that there is considerable inter-fly variability in the H1 neuron responses (Egelhaaf and Borst, 1992).

In vertebrates a segregation of pathways processing brightness increments (ON) and brightness decrements (OFF) is already found at the first synapse; between photoreceptors and bipolar cells (Kuffler, 1953). The behavioral reverse-phi phenomenon, however, shows that the motion system must recombine these pathways at some stage. Indeed, the reverse-phi property has been observed in primary visual cortex (Cat: (Emerson et al., 1987), Monkey (Livingstone and Conway, 2003)), the nucleus of

the optic tract of the wallaby (Ibbotson and Clifford, 2001), and the middle temporal area in the monkey (Livingstone et al., 2001, Krekelberg and Albright, 2005).

### 3.3.3 *Nonlinear interactions*

The multiplication of two signals is the essential nonlinearity that creates direction selectivity in the Reichardt detector (Poggio and Reichardt, 1973, Poggio and Reichardt, 1981). Such a quadratic nonlinearity predicts that a sinusoidal input signal will lead to output signals that vary at the fundamental as well as the second harmonic frequency. To be specific, for a moving grating sliding over the detector, one can split the response of the detector into three terms. The first is time independent and changes sign with the direction of motion, the second term modulates at the temporal frequency of the stimulus, and the third term modulates at twice the frequency of the stimulus (Egelhaaf et al., 1989).

In an ideal Reichardt detector the oscillations in one subunit precisely cancel those in the other subunit. But, of course, precise cancellation is a mathematical abstraction that is not truly expected in biological hardware. When stimulated with a moving grating, horizontal cells (HS) in the blowfly do show oscillations. Nearly 90% of the signal was found at or below the second harmonic frequency. This shows that the nonlinearity in the HS motion detector is indeed close to second-order. Moreover, as predicted by the Reichardt model, the oscillations at the fundamental (stimulus) frequency depended strongly on the direction of the stimulus, but the frequency-doubled responses did not (Egelhaaf et al., 1989). This confirms that the Reichardt model is a good description of the HS neuron, with the addition that the subtraction of the subunit outputs is not perfect. Typically, the

gain of the anti-preferred subunit is on the order of 0.9. This makes the motion detector suboptimal, because the equal subtraction of the two subunits maximizes direction selectivity (Borst and Egelhaaf, 1990). Moreover, this imbalance will also cause vigorous responses to flickering patterns that do not move, but whose luminance is modulated over time. This is found for many motion sensitive neurons both in invertebrate (Egelhaaf et al., 1989) and vertebrate systems (Churan and Ilg, 2002).

Interestingly, however, such imperfectly balanced and therefore suboptimal motion detection units have a reduced dependence on the spatial frequency of the stimulus. In fact, the response of a single subunit is tuned for velocity, and not temporal frequency (Zanker et al., 1999). This suggests that some visual systems could use imperfect subunit subtraction (Stage V, Figure 5) to trade-off optimal direction selectivity against spatial frequency dependence.

### *3.3.4 Shunting inhibition*

The Reichardt detector makes use of multiplication. This is a decidedly nonlinear mechanism and does not fit easily with the standard integrate and fire view of a neuron. When one takes a closer look at the biophysics of realistic neurons, however, multiplicative nonlinearities appear to be possible by a mechanism called shunting inhibition (Thorson, 1966b, Thorson, 1966a, Torre and Poggio, 1978).

Consider a model neuron with an excitatory channel and inhibitory channel. The reversal potential for the excitatory channel is typically much larger than the resting potential, which provides the depolarizing current flow of an excitatory input. The reversal

potential of the inhibitory channel, however, is assumed to be slightly above the resting potential. The two channels are organized such that preferred motion leads to temporally non-overlapping activation of the channels. For a two-flash preferred direction stimulus this arrangement will lead to a depolarizing current from the excitatory channel as well as a depolarizing current from the inhibitory channel. In other words, the response to a two-flash sequence is somewhat higher than that to a one flash sequence. Note, however, that this effect is a simple linear summation, and no difference is expected between the sum of the response to two single flashes and the response to two flashes. I.e. there is no nonlinear facilitation in this shunting inhibition model. While this may account for the limited facilitation found in direction selective cells in the rabbit retina (Barlow and Hill, 1963, Barlow et al., 1964), it is not a good model of the nonlinear facilitation observed in insects (Borst and Egelhaaf, 1990).

When motion in the anti-preferred direction is presented to the model neuron, the excitatory and inhibitory conductances are activated at the same time. Under these circumstances the inhibitory channel essentially creates a large hole in the membrane. Any current flow caused by the simultaneous activation of excitatory channels will simply seep out through this hole. In other words, this so-called shunting inhibitory channel can veto nearby excitatory currents. While this example uses a simplified model neuron, Koch et al.(1983) developed a model that incorporates the spatial extent of the dendritic tree and the relative positioning of excitatory and shunting inhibition channels. They confirmed that shunting inhibition can lead to the desired veto-effect, but found that it will only veto excitatory input if the shunt is between the excitatory input and the soma. A formal analysis shows that the efficacy of the veto is proportional to the product of the

excitatory and inhibitory conductance (Torre and Poggio, 1978). Hence, the inhibitory part of the mechanism is similar to the multiplicative nonlinear element in Reichardt's original model. It should be noted, however, that a true quadratic nonlinearity is difficult to implement with shunting inhibition under biophysically realistic assumptions (Grzywacz and Koch, 1987).

The shunting inhibition model provides a possible mechanism to implement a multiplicative nonlinearity, but what is the evidence that shunting inhibition is actually used in neural systems? Many direction selective neurons contain GABA ( $\gamma$ -aminobutyric acid) activated chloride channels whose reversal potential is close to the resting potential. In other words, the gabaergic synapse could function as a shunt. Indeed, shunting inhibition has been demonstrated directly in cat visual cortex (Borg-Graham et al., 1998, Hirsch et al., 1998). Moreover, when gabaergic synapses are inactivated pharmacologically, direction selectivity in many systems is greatly reduced (Fly: (Schmid and Bülthoff, 1988) Rabbit: (Ariel and Daw, 1982), Cat: . (Sillito, 1977)). However, one should be cautious in interpreting this as evidence in favor of the shunting inhibition model. There are many stages in the Reichardt model that require some kind of inhibition. For instance, the subtraction stage (IV in Figure 4, V in Figure 5), subtracts the outputs of the two subunits. This subtraction removes non-direction selective components from the subunits and helps create a strongly direction selective motion detector (Borst and Egelhaaf, 1990). If gabaergic synapses underlie this subtraction, then GABA antagonists would be expected to decrease direction selectivity, no matter how the multiplicative interaction were implemented.

In the fly, a clever experiment was done to distinguish such linear GABA-dependent contributions from nonlinear GABA-dependent contributions to direction selectivity. The crucial idea behind this experiment is that the multiplicative nonlinearity introduces higher harmonics in the output signal of the detector. The subtraction of the two subunits of the Reichardt detector, however, removes those components. In other words, by determining whether GABA agonists decrease or increase the higher harmonics, one can determine whether they affect the multiplicative or subtractive element of the Reichardt detector. Egelhaaf et al. (1990) showed that while GABA application decreased the overall direction selectivity of the H1 cell, the power of the second harmonic frequency increased nearly ten-fold. This clearly shows that, if the H1 cell is indeed well-described by the Reichardt model, its multiplicative stage in the fly H1 cell is unlikely to be implemented with gabaergic shunting inhibition.

#### **4 SPACE-TIME ORIENTATION**

The view of motion as the successive activation of two detectors by the same feature may work well as the basis for the study of insect vision, and some artificial motion detection systems. But, for vertebrates- and humans in particular- the distribution of detectors is nearly continuous and it is unclear which features need to be matched across which periods of time and between which detectors. Adelson and Bergen (1985) formulated a view of motion that deals with such problems and side-steps the correspondence problems associated with feature matching. They noted that a single bar, moving along a horizontal trajectory, can be represented as a slanted pattern in a space-time diagram (Figure 1). Rightward slant implies rightward motion, and leftward slant leftward motion. Moreover, the slant angle in the pattern corresponds to the speed of the motion. The slant

does not depend on the shape or features of the moving object; hence the correspondence problem essentially vanishes.

Moreover, in this view of motion, there is no fundamental difference between continuous motion and apparent motion. Figure 1B shows the space-time diagram that corresponds to the apparent motion that a bar in a modern neurophysiological experiment would typically trace out on a computer screen. A detector that detects the space-time slant corresponding to continuous motion would also respond to the apparent motion. This is an appealing property of this view of motion; not only does it provide an intuitive explanation why movies generate a sense of motion; it also validates the use of (apparent) motion on computer screens to study motion detection (Watson et al., 1986).

#### *4.1 THE MOTION ENERGY MODEL*

Adelson and Bergen developed a multi-stage spatiotemporal filtering model that could detect space-time slant with neurophysiologically realistic building blocks. The flow diagram of this so-called energy model is shown in Figure 8.

**Figure 8 The motion energy model. A) A chart of the signal flow in the model. In black are the components of the rightward selective subunit, in gray the mirror symmetric leftward selective unit. The diamonds at level II indicate spatial filtering with the filters shown in panel B. Similarly, the temporal filtering of stage III uses the filters of panel C. B) Even (solid line) and odd (dashed line) spatial filters. C) Fast (solid line) and delayed (dashed line) temporal filters.**

Each stage in this filtering model serves a specific purpose. The first stage collects light; it represents the retinal input. The second stage filters the image spatially, with one of



two spatial filters, shown in the panel B. In this particular example, the spatial filters are odd and even Gabor functions. The third stage filters the image temporally, using the filters shown in panel C. One filter's response is slower than the other, thus allowing the comparison of images at different times.

At the fourth stage, inputs from two separate pathways are summed linearly. In this particular example, the spatial and temporal filters were carefully chosen such that the fourth stage of the model would lead to slanted filters. These particular filters are said to be in quadrature relationship (one filter reaches its peak when the other goes through zero) (Watson and Ahumada, 1985). While this relationship leads to the best sensitivity to motion, the only features that are essential to create space-time slant are the presence of a fast and a slow temporal filter, and spatial filters that prefer flashes in slightly different positions. Neurons at this stage modulate their response in a direction selective manner, but their time averaged response is independent of direction. This is a very general finding; a linear model cannot generate a time-averaged direction selective output (Poggio and Reichardt, 1973, Poggio and Reichardt, 1981). Stage V represents the only nonlinear element in the motion energy model; it creates a signal whose time average is direction selective. At this point in the model the average response is direction selective, but the response of the neurons still depends on the position of the moving stimulus in the cell's receptive field. This so-called phase dependence is removed in stage VI by adding two detectors with slightly different spatial properties. Based on psychophysical data obtained in humans, Adelson and Bergen added the VII-th stage to the model. At this stage, the rightward motion energy is subtracted from the leftward motion energy to

provide a single valued output that represents the perceived direction. Positive values correspond to rightward motion, negative values to leftward motion.

The name motion energy arises from a consideration of the model in Fourier terms. In a Fourier spectrogram of the luminance distribution, opposite quadrants represent motion in the same directions. Hence, to create a detector that responds to rightward motion (quadrants I and III), one first has to remove the DC components along the spatial and temporal frequency axes. Stage II and III do this. Stage IV then selectively removes signal components from quadrant II and IV. Finally, the squaring operation of stage V measures the power or energy present in the remaining signal.

## *4.2 BEHAVIORAL EVIDENCE*

Given the different components in the model, it may be somewhat surprising that - at the output level - the (extended) Reichardt detector and the motion energy model are in fact identical (van Santen and Sperling, 1985, Adelson and Bergen, 1985). As only the output of the whole detector is typically observable behaviorally, psychophysical experiments cannot distinguish between these two models. This implies that the evidence cited in favor of the Reichardt detector in Section 3.2 equally supports the Motion Energy detector.

The internal algorithms of the detectors – *how* they reach their conclusion – however, are fundamentally different. Physiological methods can probe that internal implementation of motion detection mechanisms; they are discussed in the next section.

### 4.3 *PHYSIOLOGICAL EVIDENCE*

Simulations of the motion energy model make specific predictions about the properties of cells at various stages in the model. Figure 9 shows the predicted space time response maps as assessed with one-flash stimuli. First, note that the structure of the motion-energy model at stage III (Figure 5) is identical to that of the Reichardt detector at stage III (Figure 8). Hence, the motion energy model also predicts the existence of cells with space time response maps as shown for A, B, A', and B' in Figure 6. At stage IV, however, the models diverge. Figure 9 shows the characteristic slanted response maps expected at stages IV and VI of the motion energy model.

**Figure 9 One-flash space-time response maps of the motion energy model. This figure follows the conventions of Figure 6. The space-time response maps of stage III of the motion energy model (A,B,A', B' ), are identical to those of the Reichardt model shown in Figure 6.**

The various stages of the motion energy model can be mapped quite naturally onto the visual system of cats and primates. I will review the evidence for the various stages in sequence.

#### 4.3.1 *Input from the LGN*

In cats and primates, few retinal or LGN cells are direction selective, but many cells in primary visual cortex are (Hubel and Wiesel, 1959, Hubel and Wiesel, 1962). Hence, much of the research guided by the motion energy model has been devoted to determining whether a linear summation of the output of appropriate LGN cells can lead to a direction selective response in the cortex.

Cai et al. (1997) probed cat LGN receptive fields with single flashes. They showed that the space-time RFs were typically not slanted. The space time response maps resembled the outputs at stage III (A, B) shown in Figure 6. Note, however, that even though these LGN space time response maps were not slanted, they were also not *separable*. That is, their space time response map could not be written as the product of a spatial impulse response function and a temporal impulse response function. For the discussion of motion detection, however, I will ignore this and approximate them by separable functions. Qualitatively this is a good approximation.

Stage IV of the motion energy model requires inputs that are delayed with respect to each other. In the LGN of the cat, the lagged and non-lagged cell classes seem to fulfill this prediction quite well (Mastronarde, 1987b, Mastronarde, 1987a, Saul and Humphrey, 1990, Cai et al., 1997). Primate LGN also has classes of cells that are delayed with respect to each other; the magnocellular cells typically give fast, transient responses, while parvocellular cells respond with a later sustained firing rate (Marrocco, 1976, Schiller and Malpeli, 1978).

In the spatial domain, the inputs to the motion detector also need to be shifted; either in phase, or in space. A shift in phase, combining an odd and an even symmetric cell whose spatial receptive fields are in so-called quadrature, would be optimal (Figure 8B). Most cells in the LGN, however, have even symmetric spatial receptive fields; hence it will be difficult to construct an optimal motion detector from combining LGN cells. The motion energy detector, however, can also function with two receptive fields that are shifted *spatially*. Clearly, such cells are abundant in the LGN.

Given that appropriate input neurons exist in both cat and primate LGN, what is the evidence that these actually provide the input to the direction selective cells of primary visual cortex? Certainly, both lagged and non-lagged cells project to the cortex, and simple cells- especially those in layer 4B - contain subregions of the receptive field in which response properties mimic those of LGN lagged cells and other subregions that match properties of non-lagged cells (Saul and Humphrey, 1992). Moreover, some DS simple cells have been shown to receive monosynaptic inputs from lagged LGN cells (Alonso et al., 2001). However, this does not necessarily mean that all DS cells must receive their input directly from the LGN. The alternative hypothesis is that the LGN projects to non-DS simple cells and these provide the input to DS simple cells.

There is evidence that at least some DS cells follow this indirect route. Peterson et al. (2004) recorded from pairs of monosynaptically connected simple cells; one was DS, the other was not. For each cell in such a pair, they determined the space time response map and then subtracted the RF of the non-DS cell from the RF of the DS cell. Given the linearity assumptions of the motion energy model, this should result in the RF of the missing second input neuron. Peterson et al. show examples of DS simple cells in which the non-DS simple cell provides the late input component. Because such a DS simple cell receives its delayed input from another simple cell, it does not have to rely on a lagged LGN cell. This shows that a direct input from lagged LGN cells is not *necessary* for direction selectivity.

Using these same methods, Peterson et al. also showed that there is a range of time delays between the two inputs of DS cells, and most are much smaller than predicted by the original motion energy model. In the original model, the inputs were in temporal quadrature (Figure 8C). While this relationship produces an optimal detector (Watson and Ahumada, 1985), it is not necessary to create a moderate direction selectivity. In cat DS simple cells, strong direction selectivity is restored by the spike threshold nonlinearity. Taken together the evidence from the cat suggests that DS simple cells receive both direct lagged and non-lagged LGN input as well as input from other (non-DS) simple cells. The temporal delay between these inputs varies considerably across cells.

In monkey V1, De Valois et al. (1998, , 2000) investigated the source of the input signals of DS simple cells by determining the temporal profile of the response in V1 simple cells. According to the motion energy model, this temporal profile should consist of the sum of two components; one delayed with respect to the other (Figure 8C). To extract these components, De Valois et al. used principal components analysis. First, they looked at non-DS cells. These cells typically had only a single significant component and there were two clearly distinct subsets. One set of cells had a profile with a short latency and a biphasic temporal profile; the other set had a longer latency and a monophasic profile. Then, they determined the response profiles of direction selective cells. These cells had two significant input components, one matched the early biphasic profile, and the other matched the late monophasic profile of the non-DS cells. This strongly suggests that DS cells become direction selective by linear summation of the output of cells from the two distinct classes of non-DS simple cells (or their LGN inputs). Interestingly, the delay

between the temporal profiles of the two profiles corresponds closely to temporal quadrature, which suggests that these motion detectors are closer to being optimal than those in the cat (Peterson et al., 2004). In the spatial domain, the relationship between the inputs was more varied and the optimal spatial quadrature relationship between the two inputs is expected to be rare.

The two temporal profiles observed in the V1 simple cells correspond quite closely to the response properties of two anatomically identifiable subclasses of LGN cells. Magnocellular cells have short latencies and transient biphasic responses. Parvocellular cells have longer latencies and typically a monophasic sustained response. Hence, the view that arises from this work is that magnocellular and parvocellular LGN cells each have their own non-DS simple cell targets in V1. Other simple cells then sum the input from these non-DS simple cells to generate direction selectivity in the linear manner envisaged by the motion energy model.

This is controversial because anatomical, lesion, and psychophysical studies have all been used to argue that motion is processed by the magnocellular stream. Anatomical evidence shows that layer IV $\alpha$  of V1 – in which many DS cells are found – mainly receives magnocellular input (Blasdel and Fitzpatrick, 1984). The counter argument is that there is also evidence that shows strong vertical interactions within a column; hence even if the parvocellular properties cannot reach DS cells after crossing one synapse, they can after two. Second, lesion studies have been interpreted as showing a selective involvement of the magnocellular pathway in motion perception (Merigan and Maunsell, 1993), but here too there are counterexamples. Two studies have recorded from V1 cells

while reversibly inactivating magnocellular and/or parvocellular layers in the LGN (Malpeli et al., 1981, Nealey and Maunsell, 1994). These studies showed that many DS simple cells receive input from both classes of LGN neurons and that direction selectivity is often only abolished when both magnocellular and parvocellular inputs have been silenced. While this shows that a contribution of parvocellular cells to motion detection is certainly likely, it is unlikely that the roles of the magnocellular and parvocellular cells in motion detection are as symmetric as in the de Valois model. For instance, lesions of the magnocellular layers of the LGN have a greater influence on the responses of direction selective cells in the middle temporal area (Maunsell et al., 1990).

#### *4.3.2 Linear summation*

The previous section shows that signals with appropriate temporal and spatial shifts find their way into V1 simple cells. The next question is how these non-direction selective inputs are combined. The motion energy model predicts linear summation of inputs.

Many studies using extracellular recordings from cat simple cells support this view. In a typical experiment, the receptive field of a neuron is mapped with one kind of stimulus (single flashes, stationary gratings) and then the response to another kind of stimulus (drifting sine wave gratings, or two successive flashes) is predicted based on the assumption of linear response properties. Qualitatively this was already done in the first studies of simple cells in the cat visual cortex (Hubel and Wiesel, 1959) and found to account for the direction preference of some, but certainly not all cells. In later studies these statements have become more precise. It was found that the receptive field determined with flashes could predict quite well when a moving bar would elicit the largest response (i.e. when moving from an OFF to an ON region). Other features, in



particular the small response for motion in the anti-preferred direction could not be predicted from linear superposition and various schemes of nonlinear lateral facilitation and inhibition were proposed (Goodwin et al., 1975, Emerson and Gerstein, 1977b, Emerson and Gerstein, 1977a, Ganz and Felder, 1984). All of these studies, however, used extracellular recordings and they could not distinguish between nonlinear synaptic integration and nonlinear spike generation. Hence, these results left the possibility that all observed nonlinearities were in fact due to spike generation nonlinearities (Movshon et al., 1978b).

A new wave of studies in the late eighties tested the linear model. Although the authors sometimes differed in their conclusions, with the benefit of hindsight their datasets actually appear quite similar. Most measured space time response maps were slanted and corresponded with the motion energy model (Figure 9), not with the separable response maps predicted by the Reichardt detector (Figure 6). These slanted space-time RF maps could usually predict the preferred direction of a cell, but underestimated the magnitude of the directional preference (McLean and Palmer, 1989, Tolhurst and Dean, 1991, Reid et al., 1987, Reid et al., 1991). Albrecht and Geisler (1991) resolved this discrepancy by realizing that nonlinearities unrelated to direction selectivity itself, could nevertheless affect the predictions of the linear model. One nonlinearity they had recently measured was the contrast dependence of the neural response. They proposed a neuron model in which linear summation of the inputs is followed by half-wave rectification and an exponential nonlinearity. The exponent of this nonlinearity could be derived from the contrast response function of the neuron. With this model, they could explain nearly 80% of the magnitude of the direction selectivity of simple cells and later studies have

confirmed this (DeAngelis et al., 1993). While this model still leaves ~20% to be explained, this does not necessarily mean that these 20% are due to nonlinearities that are essential to the generation of direction selectivity. Instead this could be due to other contrast-related nonlinearities such as gain control (Heeger, 1992).

To really answer the question whether direction selectivity is based on linear summation, one needs to bypass the spike generation nonlinearity. Jagadeesh et al. (1993, , 1997) did this by recording intracellularly from cat simple cells. Their data provide clear evidence for three aspects of the motion energy model. First, DS simple cells sum their non-DS inputs linearly. This was shown by predicting the membrane potentials evoked by moving gratings from the linear superposition of the potentials evoked by stationary contrast modulated gratings. This prediction was highly accurate. Second, Jagadeesh et al. showed that the direction selectivity of the spike record (i.e. what would have been measured in extracellular recordings) was about three times larger than that observed in the intracellular recordings. This directly confirms the role of the spike-generation nonlinearity as an amplifier of direction selectivity (Albrecht and Geisler, 1991, McLean et al., 1994). Third, they showed that nearly all of the membrane potential could be explained by the summation of inputs from only two subunits. These subunits had non-oriented space time response maps (Kontsevich, 1995, Jagadeesh et al., 1997).

In a further test of the linear model, Priebe and Ferster (2005) measured separate space-time response map of excitatory and inhibitory conductances in DS simple cells for bright and dark bars. First, all four response maps were clearly slanted; showing that both excitation and inhibition were direction selective for both dark and bright bars. Second,

the slant in the excitatory and inhibitory maps was the same. Hence excitation and inhibition preferred the *same* direction of motion. This argues strongly against a veto-like mechanism for direction selectivity in these cells, because such a model would predict an opposite direction preference for the inhibition. Third, when and wherever the excitation was maximal, inhibition was minimal. This suggests that direction selectivity is derived in a push-pull fashion; a bright bar in an ON region of the receptive field evokes a depolarization (push) and a dark bar at the same position evokes a hyperpolarization (pull). Given the differences in timing of the push and the pull, moving stimuli receive a succession of pushes and pulls that sum linearly. Finally, a nonlinear spike generation mechanism removes subthreshold modulations and amplifies the relatively weak direction selectivity in the membrane potential (by a factor of 2-3; just above the squaring nonlinearity of the motion energy model). Together this creates a spike signal whose time-average is strongly direction selective (Priebe and Ferster, 2005).

In the monkey, tests of the motion energy model have followed a similar path. Extracellular recordings showed slanted space time response maps for DS simple cells (De Valois and Cottaris, 1998, De Valois et al., 2000, Livingstone, 1998, Conway and Livingstone, 2003). As explained above for cat simple cells, this is evidence against a Reichardt model. As was the case for cat simple cells, the space time response map could predict the preferred direction of a cell, but it underestimated the magnitude of the direction selectivity (Conway and Livingstone, 2003). To date, no intracellular recordings have been performed to determine whether the spike generation nonlinearity underlies the enhancement of direction selectivity as it does in the cat (Jagadeesh et al., 1993).

### 4.3.3 *Motion opponency*

In the final step of the motion energy model, the output of a leftward motion selective unit is subtracted from that of a rightward motion selective unit. Behavioral evidence shows that such an opponent stage must be present in the brain (Stromeyer et al., 1984). Given the description of DS simple cells in the previous section, it seems naturally to ask whether complex cells, which are thought to combine input from multiple simple cells, implement this opponent stage of motion processing.

To test this hypothesis, Emerson et al. (1992) measured space-time interaction maps in cat complex cells. These maps show the nonlinear facilitation or suppression that one flash causes in the response of a second flash. Up until the squaring stage of the motion energy model, no nonlinear interactions are predicted, but at stage VI, simulations show that the interaction maps should be slanted (Figure 10). At the opponent stage of the detector, on the other hand, the interaction maps should be separable (Remember that the opponent stage is formally identical to the Reichardt model, which has separable interaction maps at all stages). Cat complex cells have slanted spatio-temporal interaction maps (Emerson et al., 1992, Touryan et al., 2002), which is incompatible with the motion-opponent stage. Moreover, in a direct test of motion opponency, van Wezel et al. (1996) demonstrated that complex cells responses are suppressed by a stimulus moving in the anti-preferred direction, but this suppression is far from complete (~50%). In fact, the response to a stimulus consisting of two directions of motion is often well described by the average of the responses to the two directions of motion presented separately. These data suggest that complex cells are best described by stage VI of the motion energy model.

**Figure 10 Two-flash space-time interaction maps in the motion energy model. This figure follows the conventions of Figure 7.**

Macaque complex cells also have slanted interaction maps and, when combined with a squaring nonlinearity, account reasonably well for the direction selectivity to grating stimuli (Gaska et al., 1994, Livingstone, 1998, Conway and Livingstone, 2003). As in the cat, this shows that they are well described by stage VI of the motion energy model but not the opponent stage. In agreement with this, macaque V1 cells also show incomplete suppression for stimuli containing two opposing directions (Qian and Andersen, 1994). Somewhat surprisingly, macaque complex cells not only have slanted interaction maps, but also slanted space time response maps (Conway and Livingstone, 2003). This is not expected in the motion energy model (Figure 9), but an imbalance between the subunits could cause this kind of response.

Finally, Livingstone (1998) showed that many macaque V1 complex cells had a spatially offset inhibitory zone on the null side of the receptive field. Such a zone is not expected in the motion energy model, but is reminiscent of the veto model of direction selectivity in the retina (Barlow et al., 1964). To recap, in the latter view a stimulus moving into the receptive field from the null side, produces a delayed inhibition that removes the fast excitation produced when the stimulus is in the center of the receptive field. Livingstone and Conway (1998, , 2003) speculated that such delayed asymmetric inhibition could arise from an asymmetric dendritic tree. If such a tree has slow inhibitory inputs near the soma, and fast excitatory inputs on the asymmetric dendritic tree, then a stimulus moving in the anti-preferred direction (from soma to dendrites) would evoke overlapping

excitation and inhibition and lead to little activation. For a stimulus moving from the dendrites towards the soma, on the other hand, the excitatory input would reach the soma and evoke spikes before the somatic inhibition could stop it. Anderson et al. (1999) investigated this hypothesis by a combination of physiology, anatomical reconstruction of single neurons, and modeling. First, they showed that the asymmetry of a dendritic tree did not predict the cells preferred direction. Second, their compartmental model showed that the delays that can be generated within a typical single dendritic tree were too short to explain sensitivity to slow motion. This suggests that the contribution of asymmetric inhibition to direction selectivity in the monkey is small.

The main projection area of DS complex cells in the macaque is the middle temporal area. Many of these cells reduce their response below the spontaneous firing rate when stimulated in the anti-preferred direction (Maunsell and Van Essen, 1983, Albright, 1984). While this shows the presence of some opponent mechanisms, there is no clear evidence for an opponent stage as predicted by the motion energy model. First, space-time interaction maps in MT are slanted, and not space-time separable (Livingstone et al., 2001, Pack et al., 2006). The similarity between the interaction maps of MT cells and V1 complex cells suggests that the former simply sum the output of the latter (Pack et al., 2006). Second, even in MT the suppression of the response to a preferred stimulus by an anti-preferred stimulus is far from complete (Snowden et al., 1991, Qian and Andersen, 1994). Rather than a linear subtraction of opponent responses, the interaction of multiple directions of motion may be described more accurately as a (non-linear) competition among multiple spatial and temporal frequency components (Krekelberg and Albright, 2005).

## 5 SPACE-TIME GRADIENTS

Models building on the principle of space-time gradients start from the observation that spatial and temporal change must coincide in an image to produce motion. This insight leads to a measure of velocity in an image ( $I$ ) that is defined as the ratio of the temporal and spatial change:

$$V(x,t) = \frac{\left(\frac{\partial I}{\partial t}\right)}{\left(\frac{\partial I}{\partial x}\right)}$$

Mathematically, this measure defines the true velocity at every point in space and time. This is quite different from the outputs of the Reichardt and Motion Energy detector, which do not signal the same velocity for every spatial pattern (See 3.2.4). Moreover, because a contrast change will affect both the numerator and the denominator of the gradient model, the velocity estimate does not depend on the contrast of the image. In other models, such contrast-invariance is commonly built-in after motion estimation by processes of normalization and gain control (Heeger, 1992). Mathematically, therefore, this model truly is a better estimator of velocity. The question is, however, whether this estimate is used by the brain.

The biggest challenge for the model is that velocity becomes ill-defined in regions where the spatial gradient is zero. A number of solutions have been proposed to circumvent this problem. First, one can find regions with spatial change (edges) and only then determine the ratio in a second processing stage (Marr and Ullman, 1981). Other alternatives are to include higher-order spatio-temporal derivatives - one of which will likely be non-zero-

(Johnston et al., 1992), or to pool velocity estimates over space -the estimate will be well-defined for at least some positions (Heeger and Simoncelli, 1994).

The elementary computation required in this model is differentiation. While at first somewhat difficult to imagine, differentiation is easy to implement with simple neural elements. Consider a standard ON center neuron. Its output can be described as the weighted sum of its inputs. If we assume the receptive field is a bell-shaped function (for instance a Gaussian), we can write its output as  $G * I$ , the weighted sum of the image with the receptive field. The gradient model requires outputs that are related to  $dI/dx$ , for instance  $G * dI/dx$ . Because this neuron's output is linear, the order of the weighted sum and differentiation operations does not matter:  $G * dI/dx = dG/dx * I$ . In other words an output proportional to the derivative of the image can be obtained from a simple linear neuron whose receptive field is shaped like the derivative of a bell-shaped function. Higher order derivatives can be computed using increasingly complex receptive field structures (Koenderink and van Doorn, 1987). Looking at the spatial filters in the motion energy model (Figure 8) they are reasonably well described as each other's derivatives. The same is true for the temporal filters. In other words, the motion energy model implicitly relies on spatial and temporal derivatives. By reformulating the models, it can actually be shown that some variants of the gradient models are formally equivalent to motion energy models (Heeger and Simoncelli, 1994, Bruce et al., 2003).

## 5.1 BEHAVIORAL EVIDENCE

Given that some gradient schemes are formally equivalent to correlation and energy schemes for restricted classes of stimuli, it is difficult to distinguish among these schemes using behavioral methods. In line with this, Johnston et al. have demonstrated that many



motion phenomena that have been interpreted in favor of the space-time correlation or orientation schemes, such as reverse-phi, are also found in their variant of the gradient scheme (Johnston et al., 1992).

An attractive property of the gradient model, which is not found in the other schemes, is that it accounts quite naturally for some second-order motion percepts (Johnston and Clifford, 1995a, Johnston et al., 1999, Benton et al., 2001). Correlation or energy based schemes need to hypothesize a separate rectification stage for the processing of second-order motion. (Chubb and Sperling, 1988, Chubb and Sperling, 1989, Cavanagh and Mather, 1989) [See also Chapter XX by Sperling].

In a perfect gradient model, the velocity estimate does not depend on the (spatial frequency of the) visual pattern. As discussed in 3.2.4, however, both insect and human motion perception shows signs of pattern dependence. It is not clear whether an imperfect implementation of the gradient scheme could account for this.

## 5.2 *PHYSIOLOGICAL EVIDENCE*

The gradient model has not received as much physiological attention as the other models. The reason for this may be that the behavioral evidence suggests that motion perception is not as perfect as the gradient model could be. In a few studies in the fly, however, the gradient model was explicitly compared to the Reichardt detector and the data clearly speak in favor of the latter. To wit, both the spike output (Egelhaaf et al., 1989) and dendritic calcium concentrations (Haag et al., 2004) of the direction selective H1 neuron show clear (non-direction selective) modulations that follow the intensity modulations of the input. Moreover, both response measures are tuned for a particular temporal

frequency and not a true velocity (Pattern dependence; see Section 3.2.4). These imperfections in the H1 neuron indicate that it does not use the gradient scheme to detect motion.

Johnston (1992) has proposed a biologically plausible way to implement the gradient scheme in the biological hardware of primary visual cortex. Johnston's solution to the problem of ill-defined velocities in image regions without luminance change is to determine a series expansion of the image. The best least-squares estimate of the velocity is then given by:

$$V = T/S$$

$$T = \frac{\partial^2 I}{\partial x^2} \frac{\partial^2 I}{\partial x \partial t} + \frac{\partial^3 I}{\partial x^3} \frac{\partial^3 I}{\partial^2 x \partial t} + \dots + \frac{\partial^n I}{\partial x^n} \frac{\partial^n I}{\partial^{n-1} x \partial t}$$

$$S = \frac{\partial^2 I}{\partial x^2} \frac{\partial^2 I}{\partial x^2} + \frac{\partial^3 I}{\partial x^3} \frac{\partial^3 I}{\partial x^3} + \dots + \frac{\partial^n I}{\partial x^n} \frac{\partial^n I}{\partial x^n}$$

Each term in T and S can be implemented with differentiating filters of 2<sup>nd</sup> and higher order. Figure 11 shows a few representative examples of the space time response maps that this gradient model would require. Just as the response maps of the Reichardt detector, none of these are oriented in space-time. Clearly, there is no lack of such simple cells in primary visual cortex (Livingstone, 1998, Conway and Livingstone, 2003) and they could provide the input to a gradient motion detector. Hence, in principle, the required filters seem to be present in visual cortex. However, as discussed in section 4.3.2, many direction selective simple and even complex cells have space-time oriented response maps; those cells match the components of the motion-energy model, not those of this particular implementation of the gradient model.

**Figure 11 One-flash space-time response maps of the gradient model. This figure shows some of the differentiating filters that are required in the gradient model of Johnston et al. (1992). Conventions as in Figure 6.**

## 6 CONCLUSION

While motion itself is not a complicated phenomenon, motion detection by neural systems certainly is. The reason for this is that motion can be detected in so many different ways. Many of those detection mechanisms will not be perfect, but they may just be good enough for a particular purpose. For instance, while the gradient model may balk at the imperfections of a motion energy detector, such details may not be important when deciding whether to stay put or flee an approaching predator. This view of motion detection – as a problem with many good but suboptimal solutions – suggests a less absolutist approach to the study of motion mechanisms.

Simulations of a perfect Reichardt, motion energy, or gradient based model may appear to make strict and testable predictions, but small deviations from the ideal model can lead to significant changes in those predictions. The first factor to consider here is noise. Estimating receptive field properties such as space-time response maps and interaction maps with extracellular recordings is time consuming and even then results in relatively noisy estimates. For instance, a significant amount of noise could make the separable space-time response map of a Reichardt detector look like the slanted space-time response map of the motion energy detector. Figure 2 illustrates the basic space-time filtering properties of the three models in a similar format. Without much difficulty, the motion energy filters can be seen as a blurred version of the Reichardt filters. Similarly, with enough measurement noise, the filters of the gradient scheme would be

indistinguishable from those of the motion energy model. This shows that extracellular recordings- with their low signal to noise and the confounding influence of the unknown spike-generation nonlinearity – may be hard pushed to really distinguish between these models. At the very least it shows that a small number of positive examples for a given model will not be enough to accept it.

Apart from measurement noise, the possibility of an imperfect implementation of a motion detection scheme should also be taken into account. These imperfections sometimes lead to testable predictions (Borst and Egelhaaf, 1990), but they can also blur the lines between the models. For Figure 12, I simulated an (extended) Reichardt detector that receives its input not from odd and even Gabor spatial filters (as in Figure 7), but from two even Gabor functions with a small spatial shift. The interaction map at the level of the leftward subunit shows elements that are oriented in space-time, one of the supposedly identifying markers of the motion energy model. Certainly, the space-time slant of this simulated imperfect Reichardt detector is much less clear than that of Figure 9, as well as that measured in detail in a complex cell in the cat (Emerson et al., 1992), but it shows that the lines between the models are not as clear as one would like.

**Figure 12 An imperfect Reichardt model. This space-time interaction map was calculated from an extended Reichardt detector in which the two spatial inputs are both even symmetric, but they are shifted such that the spatial receptive fields still have significant overlap. This overlap creates space-time slant in the area indicated by the dashed rectangle. Conventions as in Figure 7.**

One can look at this issue from a quite different point of view. For the neuroscientist, models that are difficult to distinguish are a problem; they make the scientific story

harder to follow and the conclusion less forceful. From the point of view of the brain, however, multiple models with similar prerequisites may be advantageous. Consider Figure 2 again; it shows that once the essential filters for a Reichardt detector are in place, building a motion energy detector should be relatively easy. Similarly, a slightly different combination of the same filters used for the motion energy detector could function as a gradient model. This suggests that the brain may not use motion detection mechanisms based exclusively on correlation, orientation, or gradients. Instead, multiple mechanisms could contribute at the same time and side-by-side. Although such mixing of multiple mechanisms does not appeal to the modeler with a keen eye for mathematical beauty, it may be the ugly reality of the perception of motion.

## 7 FIGURE LEGENDS

Figure 1 Motion as space-time orientation. A) When a bar moves smoothly rightward over time, it traces out an oriented trapezoid in a space-time plot. B) When that same bar jumps from one place to the next (apparent motion), the space-time orientation is still clearly visible. .... 3

Figure 2 Three views of motion detection. A) The Reichardt detector makes use of sensors that are displaced in space and time with respect to each other. By multiplying their outputs (indicated by the arrows), one can create a rightward (R) or leftward (L) selective detector. B) The motion energy detector uses overlapping sensors that are sensitive to rightward (R) or leftward (L) space-time slant. C) The gradient detector uses overlapping detectors, sensitive to either spatial (S) or temporal (T) change. Adapted from (Johnston and Clifford, 1995b). .... 4

Figure 3 A beetle on a *Spangenglobus*. The beetle is glued to the black pole which holds it stationary in space. When it is lowered onto the y-maze globe, it instinctively grabs it and starts “walking” along the ridges. When it comes to a y-junction, it must make a decision to go right or left. This decision can be influenced by presenting motion in the environment. (© Freiburger Universitaetsblaetter)..... 8

Figure 4 The (Hassenstein-) Reichardt detector. The light sensors represent the beetle’s ommatidia. Signals from two neighboring ommatidia (I) are multiplied at stage III. One of the two input signals, however, is first delayed (II). The output of the multiplication stage in black is selective for rightward motion. This selectivity is enhanced in the last stage (IV) by subtracting the output of a leftward selective subunit (in gray) from that of the rightward selective subunit. .... 9

Figure 5 The extended Reichardt model. Light falling on the retina is spatially (II) and temporally filtered (III). The outputs of the four filters are then pairwise multiplied (Stage IV). As in the standard Reichardt detector, the rightward selective subunit (black) is combined with a mirror symmetric leftward selective subunit (gray), at stage V..... 14

Figure 6 One flash space-time response maps of the Reichardt model. Each of these plots shows the response of a stage in the extended Reichardt model to the presentation of a single bright flashed stimulus. Time after the stimulus runs down the vertical axis, the position of the stimulus relative to the receptive field center, is on the horizontal axis. Pixels brighter than the gray zero level (see colorbar on the right), represent an increase in the activity, dark pixels represent a decrease in activity. Within the linear model, such a decrease in firing after the presentation of a bright bar is equivalent to an increase in firing after the presentation of a dark bar. The labels in the lower left corner of each space-time response map refer to the labels in Figure 5..... 15

Figure 7 Two-flash space-time interaction maps of the extended Reichardt model. These interaction maps show which part of the response to two successive flashes is not expected based on the linear summation of the response to the two flashes presented in isolation. The time between the two flashes is on the vertical axis, the distance between the flashes on the horizontal axis. Bright pixels show a facilitating interaction, dark pixels a suppressive interaction. .... 17

Figure 8 The motion energy model. A) A chart of the signal flow in the model. In black are the components of the rightward selective subunit, in gray the mirror symmetric leftward selective unit. The diamonds at level II indicate spatial filtering with the filters shown in panel B. Similarly, the temporal filtering of stage III uses the filters of panel C. B) Even (solid line) and odd (dashed line) spatial filters. C) Fast (solid line) and delayed (dashed line) temporal filters. .... 24

Figure 9 One-flash space-time response maps of the motion energy model. This figure follows the conventions of Figure 6. The space-time response maps of stage III of the motion energy model (A,B,A', B' ), are identical to those of the Reichardt model shown in Figure 6. .... 27

Figure 10 Two-flash space-time interaction maps in the motion energy model. This figure follows the conventions of Figure 7..... 37

Figure 11 One-flash space-time response maps of the gradient model. This figure shows some of the differentiating filters that are required in the gradient model of Johnston et al. (1992). Conventions as in Figure 6..... 43

Figure 12 An imperfect Reichardt model. This space-time interaction map was calculated from an extended Reichardt detector in which the two spatial inputs are both even symmetric, but they are shifted such that the spatial receptive fields still have

significant overlap. This overlap creates space-time slant in the area indicated by the dashed rectangle. Conventions as in Figure 7..... 44

## 8 SUGGESTIONS FOR CROSS-REFERENCES

Are in the text as [See Chapter XXX by YYY].

## 9 REFERENCES

- ADELSON, E. H. & BERGEN, J. R. (1985) Spatiotemporal energy models for the perception of motion. *J Opt Soc Am A*, 2, 284-99.
- ALBRECHT, D. G. & GEISLER, W. S. (1991) Motion selectivity and the contrast-response function of simple cells in the visual cortex. *Vis Neurosci*, 7, 531-46.
- ALBRIGHT, T. D. (1984) Direction and orientation selectivity of neurons in visual area MT of the macaque. *J Neurophysiol*, 52, 1106-30.
- ALONSO, J. M., USREY, W. M. & REID, R. C. (2001) Rules of connectivity between geniculate cells and simple cells in cat primary visual cortex. *J Neurosci*, 21, 4002-15.
- AMTHOR, F. R. & GRZYWACZ, N. M. (1993) Inhibition in ON-OFF directionally selective ganglion cells of the rabbit retina. *J Neurophysiol*, 69, 2174-87.
- ANDERSON, J. C., BINZEGGER, T., KAHANA, O., MARTIN, K. A. & SEGEV, I. (1999) Dendritic asymmetry cannot account for directional responses of neurons in visual cortex. *Nat Neurosci*, 2, 820-4.
- ANSTIS, S. M. (1970) Phi movement as a subtraction process. *Vision Res.*, 10, 1411-1430.
- ANSTIS, S. M. & ROGERS, B. J. (1975) Illusory reversal of visual depth and movement during changes of contrast. *Vision Res.*, 15, 957-961.
- ARIEL, M. & DAW, N. W. (1982) Pharmacological analysis of directionally sensitive rabbit retinal ganglion cells. *J Physiol*, 324, 161-85.
- BARLOW, H. B. & HILL, R. M. (1963) Selective sensitivity to direction of movement in ganglion cells of the rabbit retina. *Science*, 139, 412-4.
- BARLOW, H. B., HILL, R. M. & LEVICK, W. R. (1964) Retinal Ganglion Cells Responding Selectively to Direction and Speed of Image Motion in the Rabbit. *J Physiol*, 173, 377-407.
- BENTON, C. P., JOHNSTON, A., MCOWAN, P. W. & VICTOR, J. D. (2001) Computational modeling of non-Fourier motion: further evidence for a single luminance-based mechanism. *J Opt Soc Am A Opt Image Sci Vis*, 18, 2204-8.
- BLASDEL, G. G. & FITZPATRICK, D. (1984) Physiological organization of layer 4 in macaque striate cortex. *J Neurosci*, 4, 880-95.
- BORG-GRAHAM, L. J., MONIER, C. & FREGNAC, Y. (1998) Visual input evokes transient and strong shunting inhibition in visual cortical neurons. *Nature*, 393, 369-73.



- BORST, A. & EGELHAAF, M. (1990) Direction selectivity of blowfly motion-sensitive neurons is computed in a two-stage process. *Proc Natl Acad Sci U S A*, 87, 9363-7.
- BRUCE, V., GREEN, P. R. & GEORGESON, M. A. (2003) *Visual Perception: Physiology, Psychology and Ecology*, Taylor & Francis, Inc.
- BUCHNER, E. (1984) Behavioural Analysis of Spatial Vision in Insects. IN ALI, M. A. (Ed.) *Photoreception and Vision in Invertebrates*. New York, Plenum Press.
- BURR, D. C. & ROSS, J. (1982) Contrast sensitivity at high velocities. *Vision Res*, 22, 479-84.
- CAI, D., DEANGELIS, G. C. & FREEMAN, R. D. (1997) Spatiotemporal receptive field organization in the lateral geniculate nucleus of cats and kittens. *J Neurophysiol*, 78, 1045-61.
- CAVANAGH, P. & MATHER, G. (1989) Motion: the long and short of it. *Spat Vis*, 4, 103-29.
- CHUBB, C. & SPERLING, G. (1988) Drift-balanced random stimuli: a general basis for studying non-Fourier motion perception. *J Opt Soc Am A*, 5, 1986-2007.
- CHUBB, C. & SPERLING, G. (1989) Two motion perception mechanisms revealed through distance-driven reversal of apparent motion. *Proc Natl Acad Sci U S A*, 86, 2985-2989.
- CHURAN, J. & ILG, U. J. (2002) Flicker in the visual background impairs the ability to process a moving visual stimulus. *Eur J Neurosci*, 16, 1151-62.
- CLIFFORD, C. W. & IBBOTSON, M. R. (2002) Fundamental mechanisms of visual motion detection: models, cells and functions. *Prog Neurobiol*, 68, 409-37.
- CONWAY, B. R. & LIVINGSTONE, M. S. (2003) Space-time maps and two-bar interactions of different classes of direction-selective cells in macaque V-1. *J Neurophysiol*, 89, 2726-42.
- DE VALOIS, R. L. & COTTARIS, N. P. (1998) Inputs to directionally selective simple cells in macaque striate cortex. *Proc Natl Acad Sci U S A*, 95, 14488-93.
- DE VALOIS, R. L., COTTARIS, N. P., MAHON, L. E., ELFAR, S. D. & WILSON, J. A. (2000) Spatial and temporal receptive fields of geniculate and cortical cells and directional selectivity. *Vision Res*, 40, 3685-702.
- DEANGELIS, G. C., OHZAWA, I. & FREEMAN, R. D. (1993) Spatiotemporal organization of simple-cell receptive fields in the cat's striate cortex. II. Linearity of temporal and spatial summation. *Journal of Neurophysiology*, 69, 1118-1135.
- EGELHAAF, M. & BORST, A. (1992) Are there separate ON and OFF channels in fly motion vision? *Vis Neurosci*, 8, 151-64.
- EGELHAAF, M., BORST, A. & PILZ, B. (1990) The role of GABA in detecting visual motion. *Brain Res*, 509, 156-60.
- EGELHAAF, M., BORST, A. & REICHARDT, W. (1989) Computational structure of a biological motion-detection system as revealed by local detector analysis in the fly's nervous system. *J Opt Soc Am A*, 6, 1070-87.
- EMERSON, R. C., BERGEN, J. R. & ADELSON, E. H. (1992) Directionally selective complex cells and the computation of motion energy in cat visual cortex. *Vision Res*, 32, 203-18.
- EMERSON, R. C., CITRON, M. C., VAUGHN, W. J. & KLEIN, S. A. (1987) Nonlinear directionally selective subunits in complex cells of cat striate cortex. *J Neurophysiol*, 58, 33-65.

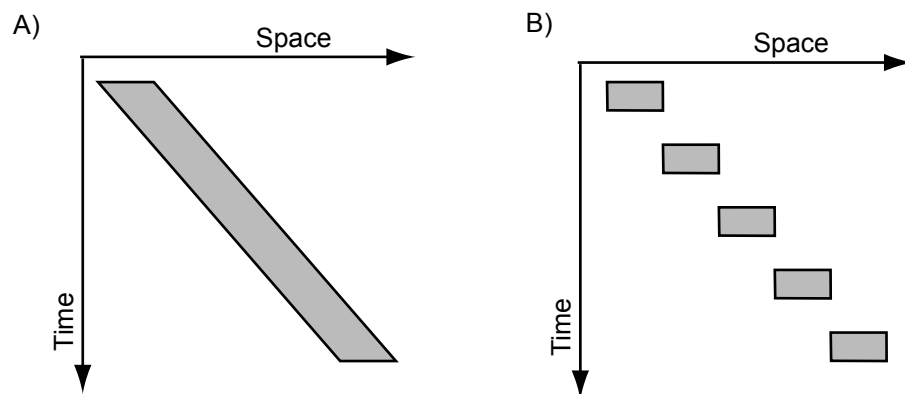
- EMERSON, R. C. & GERSTEIN, G. L. (1977a) Simple striate neurons in the cat. I. Comparison of responses to moving and stationary stimuli. *J Neurophysiol*, 40, 119-35.
- EMERSON, R. C. & GERSTEIN, G. L. (1977b) Simple striate neurons in the cat. II. Mechanisms underlying directional asymmetry and directional selectivity. *J Neurophysiol*, 40, 136-55.
- FRANCESCHINI, N., RIEHLE, A. & LE NESTOUR, A. (1989) Directionally Selective Motion Detection by Insect Neurons. IN STAVENGA, D. G. & HARDIE, R. C. (Eds.) *Facets of Vision*. Berlin Heidelberg, Springer.
- FRIED, S. I., MUNCH, T. A. & WERBLIN, F. S. (2002) Mechanisms and circuitry underlying directional selectivity in the retina. *Nature*, 420, 411-4.
- FRIED, S. I., MUNCH, T. A. & WERBLIN, F. S. (2005) Directional selectivity is formed at multiple levels by laterally offset inhibition in the rabbit retina. *Neuron*, 46, 117-27.
- GANZ, L. & FELDER, R. (1984) Mechanism of directional selectivity in simple neurons of the cat's visual cortex analyzed with stationary flash sequences. *J Neurophysiol*, 51, 294-324.
- GASKA, J. P., JACOBSON, L. D., CHEN, H. W. & POLLEN, D. A. (1994) Space-time spectra of complex cell filters in the macaque monkey: a comparison of results obtained with pseudowhite noise and grating stimuli. *Vis Neurosci*, 11, 805-21.
- GOODWIN, A. W., HENRY, G. H. & BISHOP, P. O. (1975) Direction selectivity of simple striate cells: properties and mechanism. *J Neurophysiol*, 38, 1500-23.
- GRZYWACZ, N. M. & AMTHOR, F. R. (1993) Facilitation in ON-OFF directionally selective ganglion cells of the rabbit retina. *J Neurophysiol*, 69, 2188-99.
- GRZYWACZ, N. M. & KOCH, C. (1987) Functional properties of models for direction selectivity in the retina. *Synapse*, 1, 417-34.
- HAAG, J., DENK, W. & BORST, A. (2004) Fly motion vision is based on Reichardt detectors regardless of the signal-to-noise ratio. *Proc Natl Acad Sci U S A*, 101, 16333-8.
- HASSENSTEIN, B. & REICHARDT, W. (1956) Systemtheoretische Analyse der Zeit-, Reihenfolgen und Vorzeichenauswertung bei der Bewegungsperezeption des Russelkaefers *Chlorophanus*. *Z. Naturforsch*, 11 B, 513-524.
- HEEGER, D. J. (1992) Normalization of cell responses in cat striate cortex. *Vis Neurosci*, 9, 181-97.
- HEEGER, D. J. & SIMONCELLI, E. P. (1994) Model of visual motion sensing. IN HARRIS, L. & JENKIN, M. (Eds.) *Spatial Vision in Humans and Robots*. Cambridge, Cambridge University Press.
- HIRSCH, J. A., ALONSO, J. M., REID, R. C. & MARTINEZ, L. M. (1998) Synaptic integration in striate cortical simple cells. *J Neurosci*, 18, 9517-28.
- HORRIDGE, G. A. & MARCELJA, L. (1991) A test for multiplication in insect directional motion detectors. *Philos Trans R Soc Lond B Biol Sci*, 331, 199-204.
- HUBEL, D. H. & WIESEL, T. N. (1959) Receptive fields of single neurones in the cat's striate cortex. *J Physiol*, 148, 574-91.
- HUBEL, D. H. & WIESEL, T. N. (1962) Receptive fields, binocular interaction and functional architecture in the cat's visual cortex. *J Physiol*, 160, 106-54.
- IBBOTSON, M. R. & CLIFFORD, C. W. (2001) Interactions between ON and OFF signals in directional motion detectors feeding the not of the wallaby. *J Neurophysiol*, 86, 997-1005.

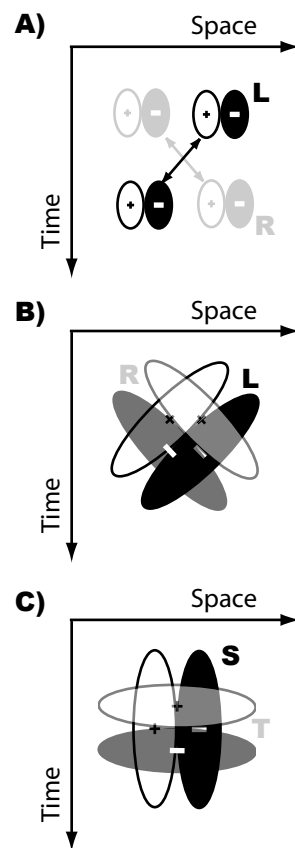
- JAGADEESH, B., WHEAT, H. S. & FERSTER, D. (1993) Linearity of summation of synaptic potentials underlying direction selectivity in simple cells of the cat visual cortex. *Science*, 262, 1901-4.
- JAGADEESH, B., WHEAT, H. S., KONTSEVICH, L. L., TYLER, C. W. & FERSTER, D. (1997) Direction selectivity of synaptic potentials in simple cells of the cat visual cortex. *J Neurophysiol*, 78, 2772-89.
- JOHNSTON, A., BENTON, C. P. & MCOWAN, P. W. (1999) Induced motion at texture-defined motion boundaries. *Proc R Soc Lond B Biol Sci*, 266, 2441-50.
- JOHNSTON, A. & CLIFFORD, C. W. (1995a) Perceived motion of contrast-modulated gratings: predictions of the multi-channel gradient model and the role of full-wave rectification. *Vision Res*, 35, 1771-83.
- JOHNSTON, A. & CLIFFORD, C. W. (1995b) A unified account of three apparent motion illusions. *Vision Res*, 35, 1109-23.
- JOHNSTON, A., MCOWAN, P. W. & BUXTON, H. (1992) A computational model of the analysis of some first-order and second-order motion patterns by simple and complex cells. *Proc R Soc Lond B Biol Sci*, 250, 297-306.
- KOCH, C., POGGIO, T. & TORRE, V. (1983) Nonlinear interactions in a dendritic tree: localization, timing, and role in information processing. *Proc Natl Acad Sci U S A*, 80, 2799-802.
- KOENDERINK, J. J. & VAN DOORN, A. J. (1987) Representation of local geometry in the visual system. *Biol Cybern*, 55, 367-75.
- KONTSEVICH, L. L. (1995) The nature of the inputs to cortical motion detectors. *Vision Res*, 35, 2785-93.
- KREKELBERG, B. & ALBRIGHT, T. D. (2005) Motion mechanisms in macaque MT. *J Neurophysiol*, 93, 2908-21.
- KUFFLER, S. W. (1953) Discharge patterns and functional organization of mammalian retina. *J Neurophysiol*, 16, 37-68.
- LIVINGSTONE, M. S. (1998) Mechanisms of direction selectivity in macaque V1. *Neuron*, 20, 509-26.
- LIVINGSTONE, M. S. & CONWAY, B. R. (2003) Substructure of direction-selective receptive fields in macaque V1. *J Neurophysiol*, 89, 2743-59.
- LIVINGSTONE, M. S., PACK, C. C. & BORN, R. T. (2001) Two-dimensional substructure of MT receptive fields. *Neuron*, 30, 781-93.
- LU, Z. L. & SPERLING, G. (1999) Second-order reversed phi. *Percept Psychophys*, 61, 1075-88.
- MALPELI, J. G., SCHILLER, P. H. & COLBY, C. L. (1981) Response properties of single cells in monkey striate cortex during reversible inactivation of individual lateral geniculate laminae. *J Neurophysiol*, 46, 1102-19.
- MARMARELIS, P. Z. & MARMARELIS, V. Z. (1978) *Analysis of Physiological Systems: The White-Noise Approach*, New York, Plenum Press.
- MARR, D. (1982) *Vision: A Computational Investigation into the Human Representation and Processing of Visual Information*, W.H. Freeman.
- MARR, D. & ULLMAN, S. (1981) Directional selectivity and its use in early visual processing. *Proc R Soc Lond B Biol Sci*, 211, 151-80.
- MARROCCO, R. T. (1976) Sustained and transient cells in monkey lateral geniculate nucleus: conduction velocities and response properties. *J Neurophysiol*, 39, 340-53.

- MASTRONARDE, D. N. (1987a) Two classes of single-input X-cells in cat lateral geniculate nucleus. I. Receptive-field properties and classification of cells. *J Neurophysiol*, 57, 357-80.
- MASTRONARDE, D. N. (1987b) Two classes of single-input X-cells in cat lateral geniculate nucleus. II. Retinal inputs and the generation of receptive-field properties. *J Neurophysiol*, 57, 381-413.
- MAUNSELL, J. H., NEALEY, T. A. & DEPRIEST, D. D. (1990) Magnocellular and parvocellular contributions to responses in the middle temporal visual area (MT) of the macaque monkey. *J Neurosci*, 10, 3323-34.
- MAUNSELL, J. H. & VAN ESSEN, D. C. (1983) Functional properties of neurons in middle temporal visual area of the macaque monkey. I. Selectivity for stimulus direction, speed, and orientation. *J Neurophysiol*, 49, 1127-47.
- MCCANN, G. D. & MACGINITIE, G. F. (1965) Optomotor response studies of insect vision. *Proc R Soc Lond B Biol Sci*, 163, 369-401.
- MCLEAN, J. & PALMER, L. A. (1989) Contribution of linear spatiotemporal receptive field structure to velocity selectivity of simple cells in area 17 of cat. *Vision Res*, 29, 675-9.
- MCLEAN, J., RAAB, S. & PALMER, L. A. (1994) Contribution of linear mechanisms to the specification of local motion by simple cells in areas 17 and 18 of the cat. *Vis Neurosci*, 11, 271-94.
- MERIGAN, W. H. & MAUNSELL, J. H. (1993) How parallel are the primate visual pathways? *Annu Rev Neurosci*, 16, 369-402.
- MORGAN, M. J. & CHUBB, C. (1999) Contrast facilitation in motion detection: evidence for a Reichardt detector in human vision. *Vision Res*, 39, 4217-31.
- MOVSHON, J. A., THOMPSON, I. D. & TOLHURST, D. J. (1978a) Receptive field organization of complex cells in the cat's striate cortex. *J Physiol*, 283, 79-99.
- MOVSHON, J. A., THOMPSON, I. D. & TOLHURST, D. J. (1978b) Spatial summation in the receptive fields of simple cells in the cat's striate cortex. *J Physiol*, 283, 53-77.
- NEALEY, T. A. & MAUNSELL, J. H. (1994) Magnocellular and parvocellular contributions to the responses of neurons in macaque striate cortex. *J Neurosci*, 14, 2069-79.
- PACK, C. C., CONWAY, B. R., BORN, R. T. & LIVINGSTONE, M. S. (2006) Spatiotemporal structure of nonlinear subunits in macaque visual cortex. *J Neurosci*, 26, 893-907.
- PETERSON, M. R., LI, B. & FREEMAN, R. D. (2004) The derivation of direction selectivity in the striate cortex. *J Neurosci*, 24, 3583-91.
- POGGIO, T. & REICHARDT, W. (1973) Considerations on models of movement detection. *Kybernetik*, 13, 223-7.
- POGGIO, T. & REICHARDT, W. (1981) Characterization of nonlinear interactions in the fly's visual system. IN REICHARDT, W. & POGGIO, T. (Eds.) *Theoretical Approaches in Neurobiology*. Cambridge, MA, MIT Press.
- PRIEBE, N. J. & FERSTER, D. (2005) Direction selectivity of excitation and inhibition in simple cells of the cat primary visual cortex. *Neuron*, 45, 133-45.
- QIAN, N. & ANDERSEN, R. A. (1994) Transparent motion perception as detection of unbalanced motion signals. II. Physiology. *J Neurosci*, 14, 7367-80.

- REICHARDT, W. (1961) Autocorrelation, a Principle for the Evaluation of Sensory Information by the Central Nervous System. IN ROSENBLITH, W. A. (Ed.) *Sensory Communication*. Cambridge, MA, MIT Press.
- REID, R. C., SOODAK, R. E. & SHAPLEY, R. M. (1987) Linear mechanisms of directional selectivity in simple cells of cat striate cortex. *Proc Natl Acad Sci U S A*, 84, 8740-4.
- REID, R. C., SOODAK, R. E. & SHAPLEY, R. M. (1991) Directional selectivity and spatiotemporal structure of receptive fields of simple cells in cat striate cortex. *J Neurophysiol*, 66, 505-29.
- SAUL, A. B. & HUMPHREY, A. L. (1990) Spatial and Temporal Response Properties of Lagged and Nonlagged Cells in Cat Lateral Geniculate Nucleus. *Journal of Neurophysiology*, 64, 206-224.
- SAUL, A. B. & HUMPHREY, A. L. (1992) Evidence of Input from Lagged Cells in the Lateral Geniculate Nucleus to Simple Cells in Cortical Area 17 of the Cat. *Journal of Neurophysiology*, 68, 1190-1208.
- SCHILLER, P. H. & MALPELI, J. G. (1978) Functional specificity of lateral geniculate nucleus laminae of the rhesus monkey. *J Neurophysiol*, 41, 788-97.
- SCHMID, A. & BÜLTHOFF, H. (1988) Using neuropharmacology to distinguish between excitatory and inhibitory movement detection mechanisms in the fly. *Calliphora erythrocephala. Biol Cybern*, 59, 71-80.
- SILLITO, A. M. (1977) Inhibitory processes underlying the directional specificity of simple, complex and hypercomplex cells in the cat's visual cortex. *J Physiol*, 271, 699-720.
- SMITH, A. T. & EDGAR, G. K. (1990) The influence of spatial frequency on perceived temporal frequency and perceived speed. *Vision Res*, 30, 1467-74.
- SNOWDEN, R. J., TREUE, S., ERICKSON, R. G. & ANDERSEN, R. A. (1991) The Response of Area MT and V1 Neurons to Transparent Motion. *Journal of Neuroscience*, 11, 2768-2785.
- SOLOMON, J. A., CHUBB, C., JOHN, A. & MORGAN, M. (2005) Stimulus contrast and the Reichardt detector. *Vision Res*, 45, 2109-17.
- STROMEYER, C. F., 3RD, KRONAUER, R. E., MADSEN, J. C. & KLEIN, S. A. (1984) Opponent-movement mechanisms in human vision. *J Opt Soc Am A*, 1, 876-84.
- TAYLOR, W. R. & VANEY, D. I. (2002) Diverse synaptic mechanisms generate direction selectivity in the rabbit retina. *J Neurosci*, 22, 7712-20.
- THORSON, J. (1966a) Small-signal analysis of a visual reflex in the locust. I. Input parameters. *Kybernetik*, 3, 41-53.
- THORSON, J. (1966b) Small-signal analysis of a visual reflex in the locust. II. Frequency dependence. *Kybernetik*, 3, 53-66.
- TOLHURST, D. J. & DEAN, A. F. (1991) Evaluation of a linear model of directional selectivity in simple cells of the cat's striate cortex. *Vis Neurosci*, 6, 421-8.
- TORRE, V. & POGGIO, T. (1978) A synaptic mechanism possibly underlying directional selectivity to motion. *Proc. Roy. Soc. Lond. (Biol.)*, 202, 409-416.
- TOURYAN, J., LAU, B. & DAN, Y. (2002) Isolation of relevant visual features from random stimuli for cortical complex cells. *J Neurosci*, 22, 10811-8.
- VAN SANTEN, J. P. & SPERLING, G. (1984) Temporal covariance model of human motion perception. *J Opt Soc Am A*, 1, 451-73.

- VAN SANTEN, J. P. & SPERLING, G. (1985) Elaborated Reichardt detectors. *J Opt Soc Am A*, 2, 300-21.
- VAN WEZEL, R. J., LANKHEET, M. J., VERSTRATEN, F. A., MAREE, A. F. & VAN DE GRIND, W. A. (1996) Responses of complex cells in area 17 of the cat to bivectorial transparent motion. *Vision Res*, 36, 2805-13.
- WATSON, A. B. & AHUMADA, A. J. (1985) Model of human visual-motion sensing. *J. Opt. Soc. Am. Part A, Optics and Image Science (Washington)*, 2, 322-342.
- WATSON, A. B., BAKER, C. L., JR. & FARRELL, J. E. (1986) Window of visibility: a psychophysical theory of fidelity in time-sampled visual motion displays. *Journal of the Optical Society of America A*, 3, 300-307.
- WEHRHAHN, C. & RAPF, D. (1992) ON- and OFF-pathways form separate neural substrates for motion perception: psychophysical evidence. *J Neurosci*, 12, 2247-50.
- ZAAGMAN, W. H., MASTEBROEK, H. A., BUYSE, T. & KUIPER, J. W. (1976) Receptive field characteristics of a directionally selective movement detector in the visual system of the blowfly. *Journal of Comparative Physiology A*, 116, 39-50.
- ZANKER, J. M., SRINIVASAN, M. V. & EGELHAAF, M. (1999) Speed tuning in elementary motion detectors of the correlation type. *Biol Cybern*, 80, 109-16.







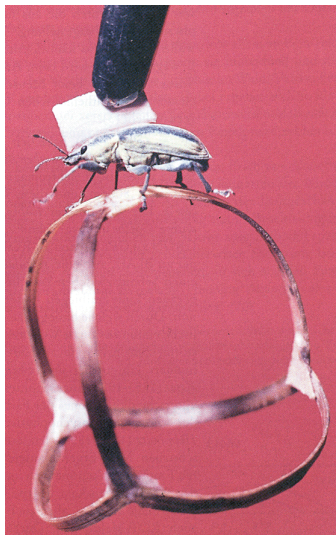


Figure 4

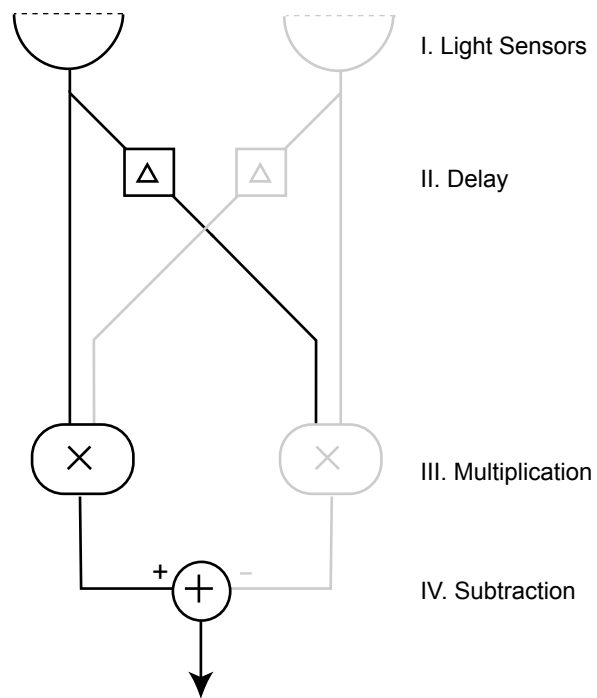


Figure 5

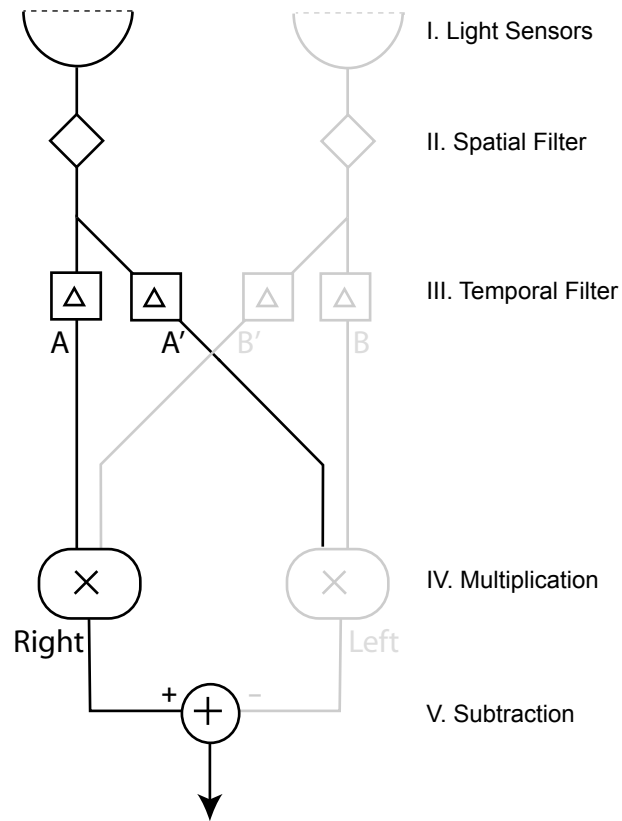
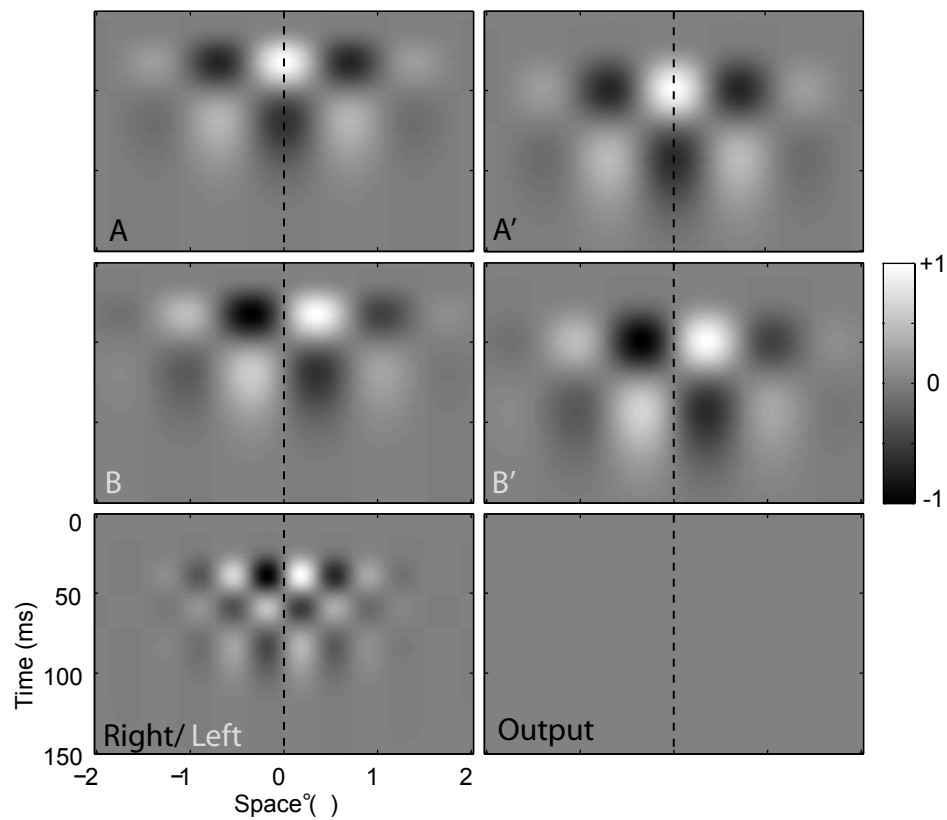


Figure 6



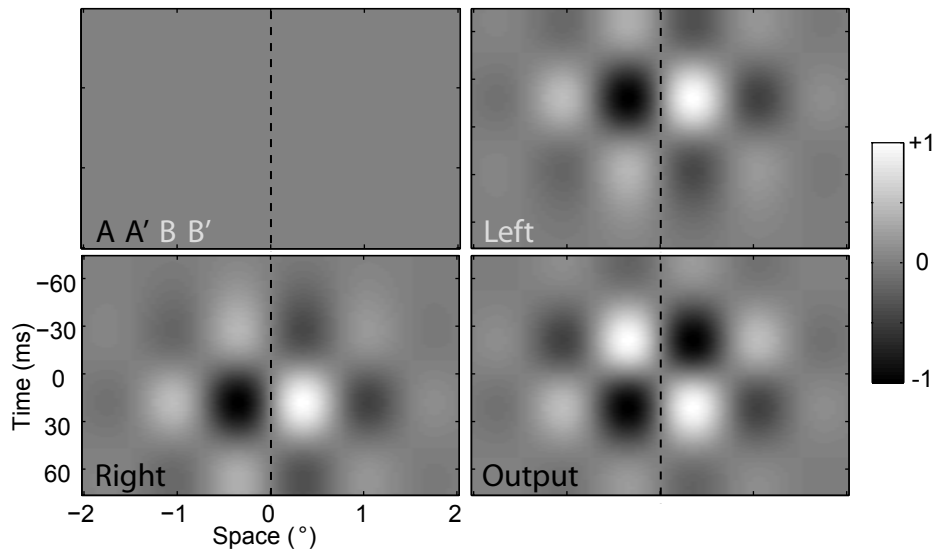


Figure 8

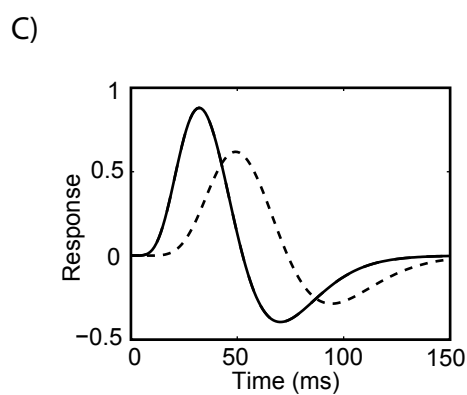
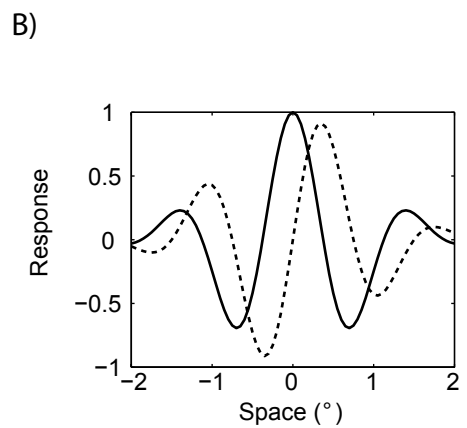
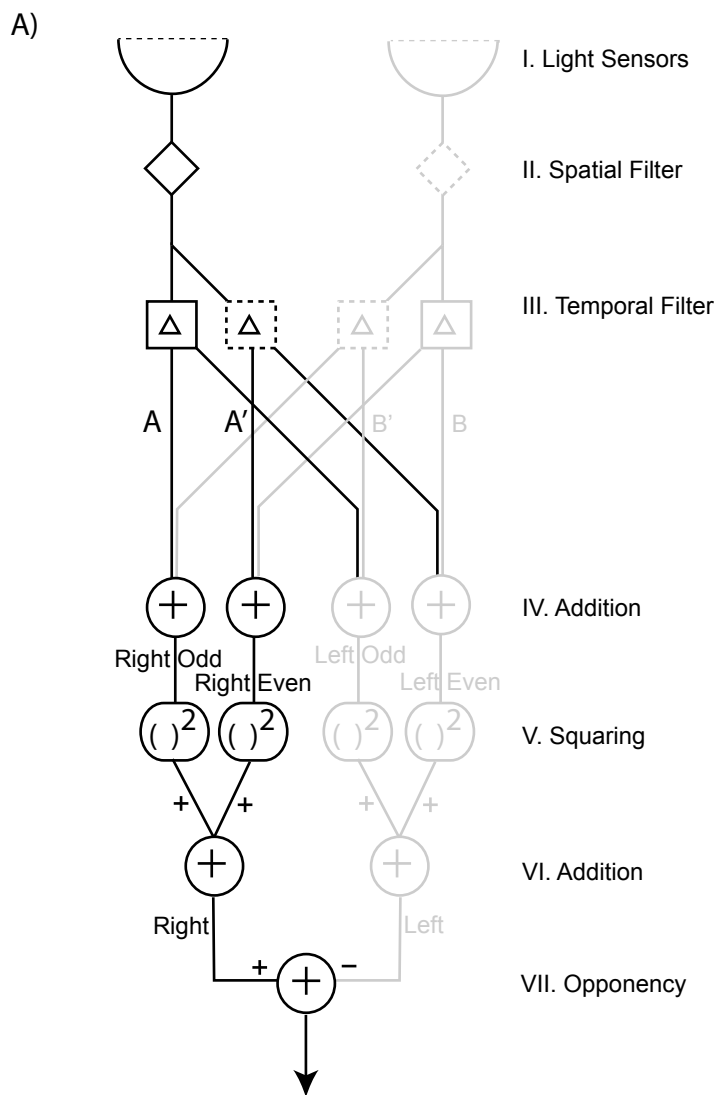


Figure 9

